

# Dependence of Intramyocardial Pressure and Coronary Flow on Ventricular Loading and Contractility: A Model Study

PETER H. M. BOVENDEERD,<sup>1</sup> PETRA BORSJE,<sup>1</sup> THEO ARTS,<sup>1,2</sup> and FRANS N. VAN DE VOSSE<sup>1</sup>

<sup>1</sup>Department of Biomedical Engineering, Eindhoven University of Technology, PO Box 513, 5600 MB, Eindhoven, The Netherlands; and <sup>2</sup>Department of Biophysics, Maastricht University, PO Box 616, 6200 MD, Maastricht, The Netherlands

(Received 5 July 2005; accepted 29 August 2006; published online: 18 October 2006)

**Abstract**—The phasic coronary arterial inflow during the normal cardiac cycle has been explained with simple (water-fall, intramyocardial pump) models, emphasizing the role of ventricular pressure. To explain changes in isovolumic and low afterload beats, these models were extended with the effect of three-dimensional wall stress, nonlinear characteristics of the coronary bed, and extravascular fluid exchange. With the associated increase in the number of model parameters, a detailed parameter sensitivity analysis has become difficult. Therefore we investigated the primary relations between ventricular pressure and volume, wall stress, intramyocardial pressure and coronary blood flow, with a mathematical model with a limited number of parameters. The model replicates several experimental observations: the phasic character of coronary inflow is virtually independent of maximum ventricular pressure, the amplitude of the coronary flow signal varies about proportionally with cardiac contractility, and intramyocardial pressure in the ventricular wall may exceed ventricular pressure. A parameter sensitivity analysis shows that the normalized amplitude of coronary inflow is mainly determined by contractility, reflected in ventricular pressure and, at low ventricular volumes, radial wall stress. Normalized flow amplitude is less sensitive to myocardial coronary compliance and resistance, and to the relation between active fiber stress, time, and sarcomere shortening velocity.

**Keywords**—Ventricular mechanics, Radial wall stress, Empty beating heart, Lumped parameter model, Intramyocardial pump.

## INTRODUCTION

Coronary arterial inflow varies in time during the cardiac cycle. Systolic inflow is smaller than diastolic inflow, demonstrating that the pulsatility of coronary flow is not caused by variation of the arterial venous pressure difference. Instead, the phasic pattern of

coronary inflow has been attributed to changes in cross-sectional area of the myocardial vessels. For example, a transient decrease in cross-sectional area affects coronary flow in two ways. First, coronary inflow decreases and outflow increases because blood is squeezed out of the coronary bed. Second, both coronary inflow and outflow decrease because of the increase of coronary resistance.

Vessel cross-sectional area depends on the local coronary pressure, the vessel wall mechanical properties and the embedment of the vessel in the myocardial tissue. The relation between vessel cross-sectional area and transmural pressure is nonlinear,<sup>11</sup> and changes due to autoregulation. The embedment in the myocardial tissue can be represented by myocardial wall stress, which consists of two contributions: the stress in the collagen matrix, through which the vessel is tied to the surrounding tissue, and the intramyocardial pressure in the interstitial fluid. In the end, the pattern of coronary flow is mainly determined by contraction of the myofibers in the cardiac wall, since myofiber contraction determines the level of both myocardial wall stress and coronary pressure.

Many experiments have been performed to elucidate the interplay between the factors governing coronary flow. It has been observed that the pulsatile component of the coronary inflow signal (1) is about proportionally related to left ventricle (LV) contractility, flow amplitude being about zero when contractility is about zero,<sup>16</sup> (2) is virtually independent of systolic LV pressure in isovolumic beats, executed at various LV volumes, for pressures up to about 13 kPa,<sup>15,17</sup> and (3) is about the same in isobaric beats at low LV pressure as in isovolumic beats at LV pressures up to about 13 kPa.<sup>15</sup> It was observed also that minimum systolic flow (4) is virtually independent of LV pressure for pressures below 13 kPa, but (5) decreases with increasing LV pressure for pressures above about 13 kPa.<sup>20</sup> In addition, it has been found that (6)

Address correspondence to Peter H. M. Bovendeerd, Department of Biomedical Engineering, Eindhoven University of Technology, PO Box 513, 5600 MB, Eindhoven, The Netherlands. Electronic mail: p.h.m.bovendeerd@tue.nl

systolic intramyocardial pressure may exceed left ventricular pressure in subendocardial layers in low afterload beats,<sup>18</sup> and (7) that an increase of coronary perfusion pressure leads to an increase of intramyocardial pressure.<sup>18</sup>

Mathematical models have been proposed as a tool to interpret the experimental data. In early models, the interaction between the coronary vessel and the myocardium was modeled through the intramyocardial pressure only. In the waterfall model<sup>9</sup> and the intramyocardial pump model,<sup>1,2,6,22</sup> this pressure was assumed to be determined completely by left ventricular pressure, with intramyocardial pressure decreasing linearly from left ventricular pressure at the endocardial surface to zero at the epicardial surface. These models can explain the pulsatility of coronary inflow under normal physiological conditions, and the experimental observations (1) and (5), listed above.

In later models, the interaction between vessel and tissue was still modeled through intramyocardial pressure only, but intramyocardial pressure was assumed to depend both on left ventricular pressure and on transverse tissue stress, i.e. stress perpendicular to the muscle fiber direction. In a finite element model of the beating heart, incorporating transverse tissue stress, observation (6) was replicated.<sup>12</sup> Transverse stress is also included in models by Beyar *et al.*, together with nonlinear characteristics of the properties of the coronary bed, and exchange of fluid between the coronary vessels and the myocardial interstitium.<sup>5,29,30</sup> In these models experimental observations (1) through (6) are replicated.

Vis *et al.*<sup>26,27</sup> extended the model for interaction between the vessel and the cardiac wall, by assuming that the coronary vessel is subject to an extravascular pressure that depends both on intramyocardial pressure and local tissue stress. So the effective compliance of the coronary vessel depends both on the compliance of the vessel wall and the stiffness of the myocardium, thus implementing an idea introduced before as the time-varying elastance concept.<sup>15,17</sup> In a finite element model of one vessel in the myocardial wall Vis *et al.* investigated the influence of contractility, pressure, and circumferential wall stretch on vessel area, for static diastole and systole. With the model, observations (6) and (7) were reproduced.

With the increasing complexity of the models, more experimental observations have been replicated. Simultaneously, the number of model parameters has increased, making it difficult to perform a detailed parameter sensitivity analysis and identify the critical model parameters. Therefore, our aim was to study the primary relations between left ventricular pressure and volume, wall stress in fiber and transverse direction, intramyocardial pressure and the coronary blood flow,

with a mathematical model with a limited number of parameters, and to assess the sensitivity of the model results to the model parameter settings.

## MATERIAL AND METHODS

The complete model consists of four parts, describing ventricular wall mechanics, myocardial constitutive properties, intramyocardial pressure, and the coronary and systemic circulation.

### *Ventricular Wall Mechanics*

The model of ventricular wall mechanics describes how left ventricular pressure and volume are related to local tissue properties, i.e. fiber stress and strain, and radial wall stress and strain. The model is based on a previously published model,<sup>3</sup> which is extended to describe the influence of radial wall stress. While the original model is derived for arbitrary ventricular geometries with rotational symmetry, here we will derive the equations for the special case of a thick walled sphere. We consider the sphere to consist of a set of nested thin spherical shells. In each shell, stresses satisfy the condition of force equilibrium in radial direction:

$$\frac{\partial \sigma_r}{\partial r} + \frac{2\sigma_r}{r} - \frac{1}{r}(\sigma_l + \sigma_c) = 0 \quad (1)$$

where  $\sigma_r$ ,  $\sigma_c$ , and  $\sigma_l$  denote the radial, circumferential and longitudinal component of the tissue stress tensor, respectively, and  $r$  indicates the radial position in the wall. We neglected shear stress components in view of the low shear stiffness of the tissue. The myocardial tissue was assumed to be incompressible, and to consist of myofibers, embedded in a collagen matrix. The Cauchy stress tensor  $\boldsymbol{\sigma}$  in tissue is written as:

$$\boldsymbol{\sigma} = -p_{im}\mathbf{I} + \boldsymbol{\sigma}_m + \sigma_a \vec{e}_f \vec{e}_f \quad (2)$$

where  $p_{im}$  denotes the intramyocardial pressure,  $\boldsymbol{\sigma}_m$ , the stress in the collagen matrix, and  $\sigma_a$  the stress generated in the myofibers along the myofiber direction  $\vec{e}_f$ . We assume that the fibers are located in spherical shells at an angle  $\alpha$  with the circumferential direction, and adopt the assumption by Arts,<sup>3</sup> that the stress in the collagen matrix in the plane of a shell is completely determined by the passive stress  $\sigma_{m,f}$  in the fibers. Then it holds:

$$\begin{aligned} \sigma_l &= -p_{im} + (\sigma_{m,f} + \sigma_a) \sin^2 \alpha = -p_{im} + \sigma_f \sin^2 \alpha \\ \sigma_c &= -p_{im} + (\sigma_{m,f} + \sigma_a) \cos^2 \alpha = -p_{im} + \sigma_f \cos^2 \alpha \\ \sigma_r &= -p_{im} + \sigma_{m,r} \end{aligned} \quad (3)$$

where  $\sigma_{m,r}$  represents the radial wall stress, generated in the collagen matrix, and the total fiber stress  $\sigma_f$  is introduced as the sum of passive and active fiber stress. Substitution in (1) yields:

$$\frac{\partial \sigma_r}{\partial r} + \frac{2\sigma_{m,r}}{r} - \frac{1}{r}\sigma_f = 0 \quad (4)$$

This equation describes how, in each shell, fiber stress  $\sigma_f$  and radial wall stress in the collagen matrix  $\sigma_{m,r}$  contribute to the variation of total radial wall stress  $\sigma_r$  in radial direction. Together, all shells increase radial wall stress from zero stress at the outer surface ( $r = r_o$ ) to minus left ventricular pressure at the inner surface ( $r = r_i$ ):

$$\sigma_r = -p_{lv} \quad \text{for } r = r_i; \quad \sigma_r = 0 \quad \text{for } r = r_o \quad (5)$$

The relation between wall stress and left ventricular pressure is found by integrating Eq. (4) from the endocardial to the epicardial surface. To evaluate the integral, we first adopt the assumption by Arts<sup>3</sup> that  $\sigma_f$  is constant across the wall. Secondly, we assume that a representative position  $\bar{r}$  can be found, such that:

$$\int_{r_i}^{r_o} d\sigma_r = \int_{r_i}^{r_o} \frac{1}{r}(\sigma_f - 2\sigma_{m,r})dr = (\sigma_f - 2\sigma_{m,r}(\bar{r})) \int_{r_i}^{r_o} \frac{1}{r}dr \quad (6)$$

Evaluation of the integral and substitution of the boundary conditions (5) yields:

$$p_{lv} = (\sigma_f - 2\sigma_{m,r}(\bar{r})) \ln\left(\frac{r_o}{r_i}\right) = \frac{1}{3}(\sigma_f - 2\bar{\sigma}_{m,r}) \ln\left(1 + \frac{V_w}{V_{lv}}\right) \quad (7)$$

where  $r_i$  and  $r_o$  are rewritten in terms of the cavity volume  $V_{lv}$  and wall volume  $V_w$ , and  $\bar{\sigma}_{m,r}$  is introduced as a short notation of  $\sigma_{m,r}(\bar{r})$ . Apart from the term  $-2\bar{\sigma}_{m,r}$ , this relation is identical to that derived in Arts et al.<sup>3</sup> To complete the model relating wall mechanics to cavity mechanics, Eq. (7) is complemented by a relation between ventricular volume and tissue strain. We choose the passive ventricle at zero transmural pressure as a reference state. In this state, we assume a sarcomere length  $l_{s0}$  and a cavity volume  $V_{lv0}$ . It has been shown,<sup>3</sup> that the fiber stretch ratio  $\lambda_f$  can be approximated by:

$$\lambda_f = \left(\frac{V_{lv} + \frac{1}{3}V_w}{V_{lv0} + \frac{1}{3}V_w}\right)^{\frac{1}{3}} \quad (8)$$

This ratio corresponds to the circumferential stretch ratio at the outer surface of a shell that contains the left ventricular cavity volume and one third of the wall

volume. At the same location, the radial stretch ratio  $\lambda_r$  equals:

$$\lambda_r = \lambda_f^{-2} \quad (9)$$

where we assumed incompressibility of the myocardial tissue. Equations (7)–(9) describe how global ventricular properties  $V_{lv}$  and  $p_{lv}$  are related to local tissue properties  $\lambda_f$ ,  $\lambda_r$ ,  $\sigma_f$  and  $\bar{\sigma}_{m,r}$ .

### Myocardial Constitutive Properties

The model of ventricular mechanics is completed with constitutive laws for fiber stress and radial stress. The active fiber stress  $\sigma_a$  was modeled to depend on contractility  $c$ , sarcomere length  $l_s$ , time elapsed since activation  $t_a$  and sarcomere shortening velocity  $v_s$  as:

$$\sigma_a(c, l_s, t_a, v_s) = c\sigma_{ar}f(l_s)g(t_a)h(v_s) \quad (10)$$

with contractility  $c$  ( $0 \leq c \leq 1$ ), scaling constant  $\sigma_{ar}$ , and:

$$f(l_s) = \begin{cases} 0 & l_s \leq l_{s,a0} \\ \frac{l_s - l_{s,a0}}{l_{s,ar} - l_{s,a0}} & l_s > l_{s,a0} \end{cases} \quad (11)$$

$$g(t_a) = \begin{cases} 0 & t_a < 0 \\ \sin^2\left(\pi \frac{t_a}{t_{max}}\right) & 0 \leq t_a \leq t_{max} \\ 0 & t_a > t_{max} \end{cases} \quad (12)$$

$$h(v_s) = \frac{1 - (v_s/v_0)}{1 + c_v(v_s/v_0)} \quad (13)$$

Here,  $l_{s,a0}$  denotes the sarcomere length below which active stress becomes zero and  $l_{s,ar}$  represents the sarcomere length to which the reference stress  $\sigma_{ar}$  is referred to. Times  $t_a$  and  $t_{max}$  denote the time elapsed since activation, and the duration of the twitch, respectively. Velocity  $v_0$  represents the unloaded sarcomere shortening velocity, while  $c_v$  governs the shape of the stress–velocity relation. Parameter values in the active stress law (Table 1) are chosen in agreement with experimental data.<sup>8,13</sup>

The passive stress along the fiber direction is modeled as:

$$\sigma_{m,f}(\lambda_f) = \begin{cases} \sigma_{f0}(\exp[c_f(\lambda_f - 1)] - 1) & \lambda_f \geq 1 \\ 0 & \lambda_f < 1 \end{cases} \quad (14)$$

where it was assumed that no stress can be transmitted in compression. Passive transverse stress is modeled similarly. Since the radial direction at ventricular level coincides with the transverse direction at the tissue

level, we write the transverse stress model in terms of radial stress and stretch ratio:

$$\sigma_{m,r}(\lambda_r) = \begin{cases} \sigma_{r0}(\exp[c_r(\lambda_r - 1)] - 1) & \lambda_r \geq 1 \\ 0 & \lambda_r < 1 \end{cases} \quad (15)$$

Settings of parameter values  $\sigma_{f0}$ ,  $c_f$ ,  $\sigma_{r0}$  and  $c_r$  are based on experimental data on the pressure volume relation of the passive left ventricle.<sup>19</sup> In the latter study, the pressure volume relation was described by a logarithmic relation, involving chamber stiffness at positive and negative pressures, and maximum and minimum attainable volume. The bottom panel of Fig. 1 shows the experimental data, and our model prediction for parameter settings in Table 1. Uniaxial stress–strain responses are shown in the top panel of Fig. 1.

### Intramyocardial Pressure

To derive the expression for the intramyocardial pressure, again we consider the ventricular wall to be composed of a number of nested shells. The pressure in between two shells is assumed to be a fraction  $\beta$  of the left ventricular pressure. In analogy to Eq. (5), this pressure is in equilibrium with radial tissue stress  $\sigma_r$ :

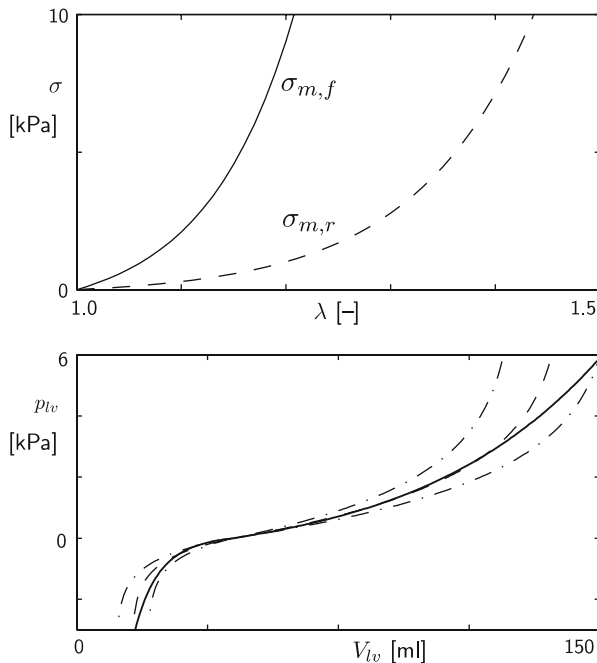


**FIGURE 1.** Passive material behavior. Top: passive stress as a function of stretch ratio  $\lambda$  for uniaxial stretch along fiber direction ( $\sigma_{m,f}$ ) and radial direction ( $\sigma_{m,r}$ ). Bottom: passive left ventricular pressure–volume relation according to model (solid line) and experimental data;<sup>19</sup> experimental data given for average minimum and maximum volume (dashed line), and minimum and maximum volume  $\pm 1$  SD (dash-dot lines).

**Table 1.** Reference settings for parameters in the model of the left ventricle.

Parameter	Value	Unit	Parameter	Value	Unit
$V_w$	200	$10^{-6} \text{ m}^3$	$\sigma_{ar}$	55	$10^3 \text{ Pa}$
$V_{lv,0}$	60	$10^{-6} \text{ m}^3$	$c$	1	–
$l_{s,0}$	1.9	$10^{-6} \text{ m}$	$l_{s,a0}$	1.5	$10^{-6} \text{ m}$
$\sigma_{f0}$	0.9	$10^3 \text{ Pa}$	$l_{s,ar}$	2.0	$10^{-6} \text{ m}$
$\sigma_{c0}$	0.2	$10^3 \text{ Pa}$	$t_{max}$	400	$10^{-3} \text{ s}$
$c_f$	12	–	$v_0$	10	$10^{-6} \text{ m s}^{-1}$
$c_r$	9	–	$c_v$	0	–

$$\sigma_r = -p_{im} + \sigma_{m,r} = -\beta \cdot p_{lv} \quad (16)$$

In the model, we assume a linear variation of  $\beta$  with the transmural position in the wall, with  $\beta = 1$  at the endocardial surface, and  $\beta = 0$  at the epicardial surface. Again stress at the shell containing the LV cavity volume and one third of LV wall volume is considered representative. For this location at a radius  $\bar{r}$  in the wall we find:

$$p_{im}(\bar{r}) = \bar{\sigma}_{m,r} + \frac{r_o - \bar{r}}{r_o - r_i} p_{lv} = \bar{p}_{im} \quad (17)$$

where we introduced the notation  $\bar{p}_{im} = p_{im}(\bar{r})$  and the radial positions  $r_i$ ,  $r_o$  and  $\bar{r}$  are defined as:

$$r_i = \left( \frac{3V_{lv}}{4\pi} \right)^{\frac{1}{3}}; \quad r_o = \left( \frac{3(V_{lv} + V_w)}{4\pi} \right)^{\frac{1}{3}}; \quad \bar{r} = \left( \frac{3(V_{lv} + V_w/3)}{4\pi} \right)^{\frac{1}{3}} \quad (18)$$

Equation (17) describes intramyocardial pressure as a function of LV pressure and volume: the volume dependency enters the equation through the radial stress  $\sigma_{m,r}$  [Eq. (15)], which depends the radial stretch ratio  $\lambda_r$  [Eq. (9)], which in turn depends on LV volume [Eq. (8)].

### Systemic and Coronary Circulation

The model of left ventricular wall mechanics is incorporated in lumped parameter models for the coronary and systemic circulation (Fig. 2). The aortic (AV) and mitral valve (MV) are modeled as an ideal diode. Vessels are modeled with constant resistances  $R$ , inertances  $L$  and capacitances  $C$ . The pressure drop  $\Delta p$  across each of these components is given by

$$\Delta p_C = \frac{V - V_0}{C} \quad (19)$$

$$\Delta p_R = Rq \quad (20)$$

$$\Delta p_L = L \frac{dq}{dt} \quad (21)$$



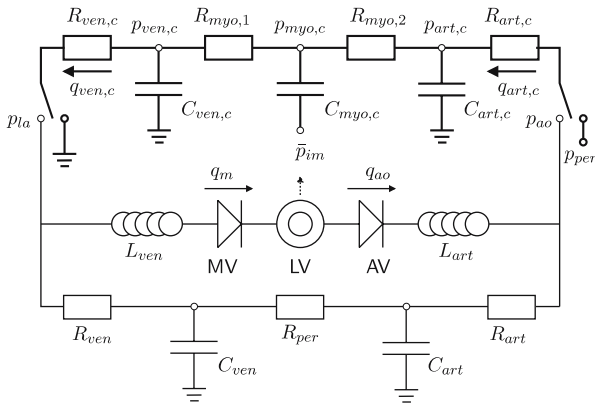


**FIGURE 2.** Schematic representation of the left ventricle (LV) in the systemic circulation and coronary circulation;  $R_{art}$ ,  $R_{per}$  and  $R_{ven}$  represent the systemic arterial, peripheral and venous resistance, respectively; MV and AV represent the mitral and aortic valve, respectively;  $C_{art}$  and  $C_{ven}$  the systemic arterial and venous compliance;  $L_{ven}$  and  $L_{art}$  the inertia of the blood in the venous and arterial system;  $R_{art,c}$ ,  $R_{myo,1}$ ,  $R_{myo,2}$  and  $R_{ven,c}$  represent the coronary arterial, the two intramyocardial and venous resistances;  $C_{art,c}$ ,  $C_{myo,c}$  and  $C_{ven,c}$  the coronary arterial, intramyocardial and venous compliance;  $p_{art,c}$ ,  $p_{myo,c}$  and  $p_{ven,c}$  the pressure in the coronary arteries, myocardium and veins, respectively;  $p_{ao}$  and  $p_{la}$  the aortic and left atrial pressure, respectively;  $q_{ao}$ ,  $q_m$  represent the AV flow and MV flow;  $q_{art,c}$  and  $q_{ven,c}$  the coronary arterial inflow and venous outflow;  $\bar{p}_{im}$  represents the intramyocardial pressure at the representative radial position  $\bar{r}$ . When simulating isovolumic and isobaric contractions, the pressure drop across the coronary circulation is switched from  $p_{ao} - p_{la}$  to a constant perfusion pressure  $p_{per}$ .

with  $V$  the volume in the capacitance and  $q$  the flow through a resistance or an inertance. The pressure–volume relation of the capacitance represents a linearization around the physiologic working point,  $V_0$  representing the volume at zero pressure. Values of parameters in the circulation model were based on literature (Table 2).

The connection between the model of LV mechanics and the coronary circulation model is made through the intramyocardial pressure, that acts on the myocardial capacitance  $C_{myo,c}$ . The values of the coronary capacitances were based on measurements by Spaan *et al.*:<sup>23</sup>

0.0022, 0.091 and 0.045 ml mm Hg<sup>-1</sup> 100 g<sup>-1</sup> LV in large coronary arteries, myocardial coronary bed, and coronary veins, respectively. Zero pressure volumes were chosen such that under normal physiological conditions, time-averaged coronary volume was about 15 ml 100 g<sup>-1</sup> of LV tissue, distributed over arterial, myocardial and venous vessels in a ratio of 1:2:2.<sup>23</sup>

In the coronary circulation, resistance values during normoxia and hyperemia were derived from Chilian *et al.*<sup>7</sup> In that study, total coronary resistance under normal and vasodilated conditions was measured to be 66 and 14 mm Hg min g ml<sup>-1</sup>, respectively. Distribution of resistance over the arterial, myocardial and venous compartment was measured to be 25, 68 and 7% under normal conditions, and 42, 27 and 31% under maximal vasodilation.

Systemic parameters are chosen to yield representative function curves for a 70 kg adult, at a heart rate of 75 bpm. LV wall volume was set to 200 ml, and cavity volume at zero pressure was set to 30% of this volume. The arterial load was modeled by a three-element windkessel model, consisting of a characteristic aortic impedance  $R_{art}$ , an arterial compliance  $C_{art}$ , and a peripheral resistance  $R_{per}$ . The peripheral resistance was chosen to yield realistic time-averaged values of aortic pressure and aortic flow. Next, arterial capacitance was chosen to yield realistic values of minimum and maximum aortic pressure. Total blood volume was set to 5000 ml. The blood volume at which mean systemic pressure is zero was assumed to be equal 70% of total blood volume, about 85% of which is contained in the venous system. Venous capacitance was chosen such that the additional 30% of blood volume leads a mean systemic pressure of about 2 kPa.

### Simulations Performed

With the model, a number of simulations were performed. First we considered the normal physiological situation, with normal vessel tone and coronary

**Table 2.** Reference settings for parameters in the circulation model; coronary resistance values in parentheses represent maximum vasodilation.

Systemic circulation			Coronary circulation		
Parameter	Value	Unit	Parameter	Value	Unit
$R_{art}$	5	10 <sup>6</sup> Pa s m <sup>-3</sup>	$R_{art,c}$	700 (200)	10 <sup>6</sup> Pa s m <sup>-3</sup>
$R_{per}$	120	10 <sup>6</sup> Pa s m <sup>-3</sup>	$R_{myo,1}$	900 (100)	10 <sup>6</sup> Pa s m <sup>-3</sup>
$R_{ven}$	5	10 <sup>6</sup> Pa s m <sup>-3</sup>	$R_{myo,2}$	900 (100)	10 <sup>6</sup> Pa s m <sup>-3</sup>
$C_{art}$	20	10 <sup>-9</sup> m <sup>3</sup> Pa <sup>-1</sup>	$R_{ven,c}$	200	10 <sup>6</sup> Pa s m <sup>-3</sup>
$C_{ven}$	800	10 <sup>-9</sup> m <sup>3</sup> Pa <sup>-1</sup>	$C_{art,c}$	0.03	10 <sup>-9</sup> m <sup>3</sup> Pa <sup>-1</sup>
$V_{art,0}$	500	10 <sup>-6</sup> m <sup>3</sup>	$C_{myo,c}$	1.4	10 <sup>-9</sup> m <sup>3</sup> Pa <sup>-1</sup>
$V_{ven,0}$	3000	10 <sup>-6</sup> m <sup>3</sup>	$C_{ven,c}$	0.7	10 <sup>-9</sup> m <sup>3</sup> Pa <sup>-1</sup>
$L_{art}$	60	10 <sup>3</sup> Pa s m <sup>-3</sup>	$V_{art,c0}$	6	10 <sup>-6</sup> m <sup>3</sup>
$L_{ven}$	60	10 <sup>3</sup> Pa s m <sup>-3</sup>	$V_{myo,c0}$	7	10 <sup>-6</sup> m <sup>3</sup>
$V_{blood}$	5000	10 <sup>-6</sup> m <sup>3</sup>	$V_{ven,c0}$	10	10 <sup>-6</sup> m <sup>3</sup>

flow driven by the difference between aortic and left atrial pressure. Next we investigated the changes induced in the isolated heart setup used by Krams *et al.*,<sup>16,17</sup> by the combination of maximum vasodilation, constant perfusion pressure and zero coronary outflow pressure. Then, under these conditions we simulated isovolumic and isobaric beats, for various settings of LV volume, pressure and contractility. Following Krams *et al.*<sup>16,17</sup> and Pagliaro *et al.*,<sup>20</sup> results were analyzed in terms of minimal systolic coronary flow  $\hat{q}_{art,c,min}$  and the normalized coronary flow amplitude (NFA):

$$NFA = \frac{\hat{q}_{art,c,max} - \hat{q}_{art,c,min}}{\hat{q}_{art,c,max}} \quad (22)$$

Finally, we investigated sensitivity of NFA to changes in myocardial radial stiffness, active material properties, coronary myocardial resistance, and coronary capacitance.

## RESULTS

### *The Normal Beating Heart*

To illustrate the behavior of the model, first the normal physiological situation was simulated, with normal vessel tone and coronary flow driven by the difference between aortic and left atrial pressure. Ventricular and intramyocardial pressure rise to 16.1 and 9.1 kPa, respectively (Fig. 3, left panel). Intramyocardial pressure is almost completely determined by ventricular pressure, since radial wall stress is virtually zero. Maximum aortic and mitral flow are 646 and 307 ml/s, respectively. Stroke volume is 75.6 ml at an ejection fraction of 64%. Perfusion pressure equals aortic pressure and varies between 11.4 and 16.3 kPa. Myocardial coronary pressure varies between 3.0 and 12.3 kPa. Left atrial pressure remains about constant at 1.45 kPa. Mean coronary arterial inflow and venous outflow are  $2.2 \text{ ml s}^{-1} 100 \text{ g}^{-1}$  LV wall volume. Coronary arterial inflow displays a two peaked pattern, the peaks occurring in early filling and in ejection. Diastolic inflow is larger than systolic inflow. Coronary arterial outflow shows only one peak per cycle, occurring during ejection. Myocardial coronary volume varies between 10.7 and 12.5 ml.

### *Constant Perfusion Pressure and Maximal Vasodilation*

This simulation represents the experimental situation in the isolated heart with a constant perfusion pressure of 10 kPa and maximal vasodilation.

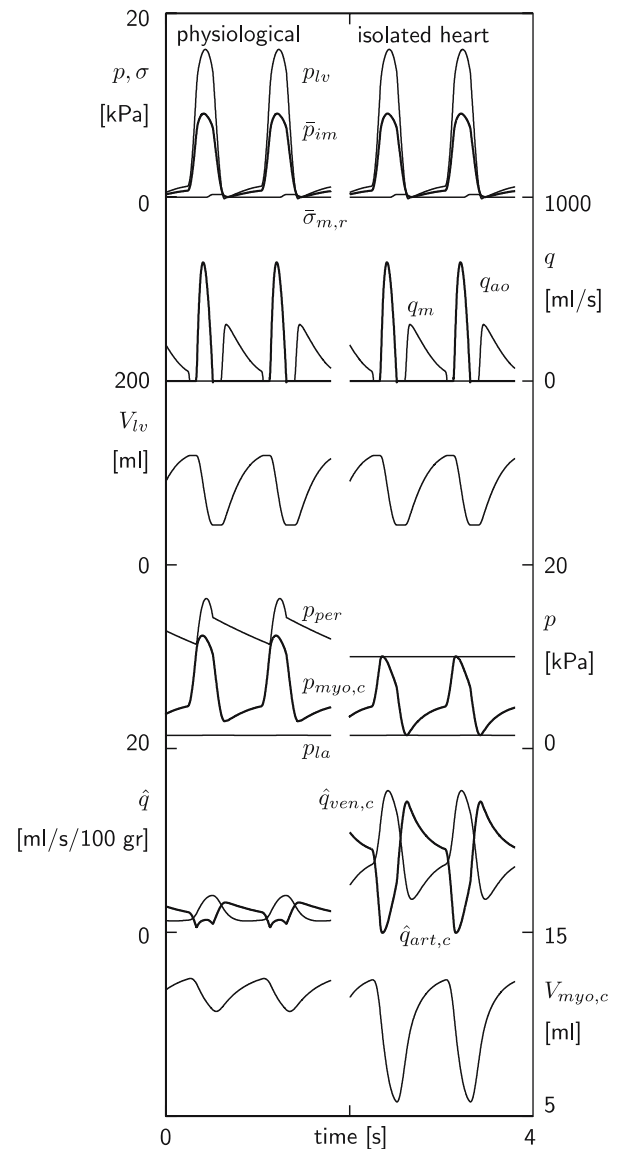


**FIGURE 3. Hemodynamics in the beating heart. Left: simulation of the physiological state with aortic pressure driving the coronary circulation. Right: simulation of isolated heart experiment with a constant perfusion pressure and maximum vasodilation. From top to bottom: ventricular pressure  $p_{lv}$ , intramyocardial pressure  $\bar{p}_{im}$  (bold) and radial wall stress  $\bar{\sigma}_{m,r}$ ; aortic valve (AV) flow  $q_{ao}$  (bold) and mitral valve (MV) flow  $q_m$ ; left ventricular cavity volume  $V_{lv}$ ; coronary perfusion pressure  $p_{per}$ , myocardial coronary pressure  $p_{myo,c}$  (bold) and left atrial pressure  $p_{la}$ ; coronary inflow  $\hat{q}_{art,c}$  (bold) and outflow  $\hat{q}_{ven,c}$  per 100 g wall volume; volume of myocardial coronary bed  $V_{myo,c}$ .**

Myocardial coronary pressure varies between 1.5 and 10.0 kPa (Fig. 3, right panel). Arterial inflow varies between  $-0.1$  and  $14.2 \text{ ml s}^{-1} 100 \text{ g}^{-1}$  LV wall volume, with a mean of  $8.3 \text{ ml s}^{-1} 100 \text{ g}^{-1}$  LV wall volume. In the arterial inflow curve, the positive flow peak in early systole has disappeared. Myocardial coronary volume varies between 5.8 and 12.4 ml.

### The Isovolumic Beating Heart

The isovolumic experiments by Krams *et al.*<sup>15–17</sup> were simulated at a constant perfusion pressure of 10 kPa and maximal vasodilation. Maximum LV pressure decreases with decreasing LV volume (Fig. 4, left panel). As LV volume decreases below 60 ml, the volume at which pressure in the passive LV is zero, diastolic LV pressure becomes negative. At these volumes, radial wall stress becomes positive, while being constant during a beat. With decreasing volume, maximum intramyocardial pressure and coronary arterial inflow decrease, whereas minimum coronary arterial inflow increases.

The normalized coronary flow amplitude (NFA) [Eq. (22)] decreases with decreasing LV pressure (Fig. 5, top left panel), but pulsatility persists at zero ventricular pressure. NFA decreases with decreasing contractility as well. Minimum coronary arterial inflow increases with decreasing LV pressure (Fig. 5, bottom left panel). At low pressures, the slope of the pressure–flow relation decreases.

For a constant LV volume of 60 ml, developed LV pressure decreases with decreasing contractility (Fig. 4, middle panel). At this volume of 60 ml, radial wall

stress is zero. Maximum intramyocardial pressure decreases with maximum LV pressure. Maximum coronary arterial inflow decreases slightly, whereas minimum coronary arterial inflow increases strongly. With decreasing contractility, normalized coronary flow amplitude (NFA) decreases about linearly, while minimal arterial inflow increases linearly (Fig. 5, middle panel). For other volumes, a similar behavior is found.

### The Isobaric Beating Heart

Simulations of hemodynamics in the isobaric beating heart were performed at a filling pressure of 1 kPa, a constant perfusion pressure of 10 kPa, maximal vasodilation and contractility parameter  $c = 1$ . With decreasing LV pressure during ejection, minimal LV volume decreases and radial wall stress increases (Fig. 4, right panel). Reduction of maximum LV pressure from 16 to 12 kPa is accompanied by a reduction of maximum intramyocardial pressure to 7.6 kPa. Maximum arterial inflow decreases, whereas minimum arterial inflow increases. Further reduction of LV pressure below 12 kPa hardly affects maximum intramyocardial pressure, due to the increasing

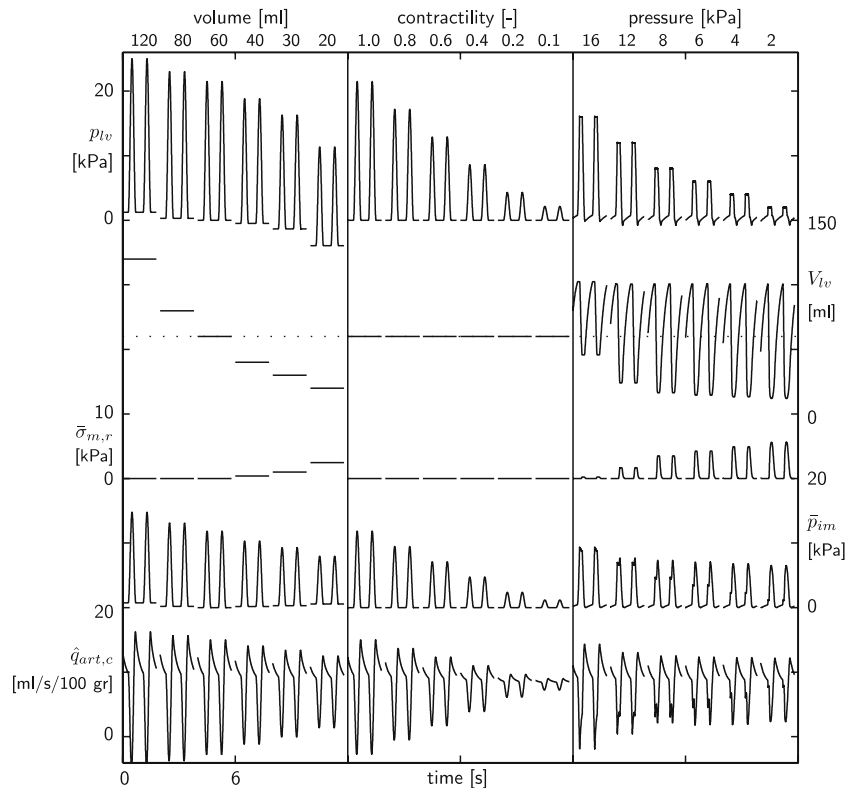


**FIGURE 4.** Hemodynamics at maximal vasodilatation and constant perfusion pressure, expressed in time courses of ventricular pressure  $p_{lv}$ , ventricular volume  $V_{lv}$ , radial wall stress  $\bar{\sigma}_{m,r}$ , intramyocardial pressure  $\bar{p}_{im}$  and coronary arterial inflow  $\hat{q}_{art,c}$ . Left: isovolumic beats for ventricular volumes ranging from 120 to 20 ml. Middle: isovolumic beats at 60 ml for contractility parameter  $c$  ranging from 1.0 to 0.1. Right: isobaric beats for systolic pressures ranging from 16 to 2 kPa.

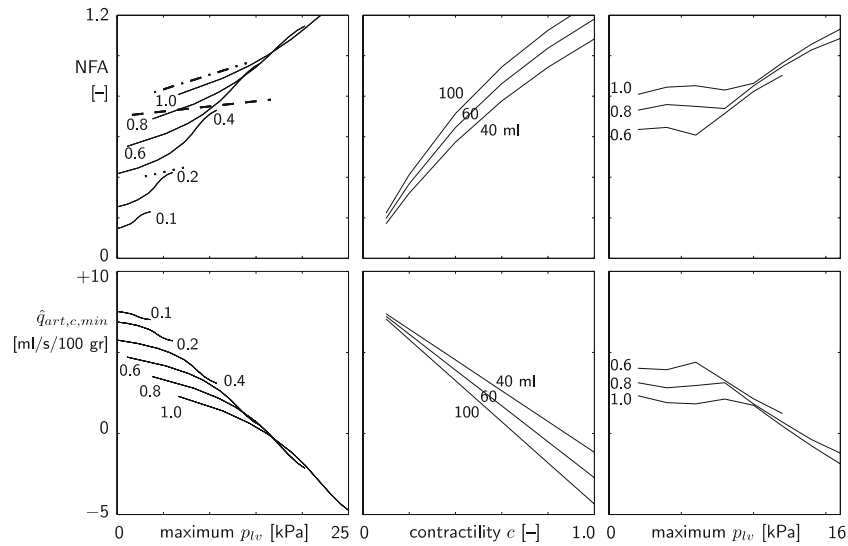


**FIGURE 5.** Analysis of coronary inflow data from simulations in Fig. 4, expressed in normalized arterial coronary flow amplitude (NFA), defined in Eq. (22), and minimal coronary arterial inflow  $\dot{q}_{art,c,min}$  in isovolumic beats as a function of maximum left ventricular pressure for contractility parameter  $c$  varying from 0.1 to 1.0; in top panel experimental data<sup>15</sup> are given by the dashed line (reference), dash-dotted line (high contractility) and dotted line (low contractility). Middle: NFA and  $\dot{q}_{art,c,min}$  in isovolumic beats as a function of contractility parameter  $c$  for LV volumes of 40, 60, and 100 ml. Right: NFA and  $\dot{q}_{art,c,min}$  in isobaric beats as a function of maximum ventricular pressure for contractility parameter  $c$  ranging from 0.6 to 1.0.

contribution of radial wall stress. Maximum and minimum arterial inflow remain about constant. These changes are reflected in the right panel of Fig. 5. With decreasing left ventricular pressure, initially NFA decreases and minimum arterial inflow increases. Below a threshold pressure of about 10 kPa, these quantities become about constant. A similar behavior is found for lower contractilities.

### Sensitivity Analysis

Results of the sensitivity analysis are shown in Fig. 6. Sensitivity to settings of parameters in the model for radial wall stress was investigated, since in our model radial wall stress is an important determinant of intramyocardial pressure. If the radial stress parameter  $c_{r0}$  [Eq. (15)] is decreased or increased by a factor 2, the pulsatile character of the coronary inflow at lower pressures persists, both for isovolumic and isobaric beats (Fig. 6, top panel). In isovolumic beats, maximum LV pressure increases with decreasing  $c_{r0}$ . At the lowest LV volume simulated, 15 ml, maximum left ventricular pressure does not drop below 14 kPa, when  $c_{r0}$  is set to zero. In isobaric beats, at high pressures NFA is not affected by changes in  $c_{r0}$ . Below an ejection pressure of 10 kPa, NFA increases with increasing radial stiffness. When  $c_{r0}$  is set to zero NFA decreases proportionally with left ventricular pressure, until pulsatility is lost at zero left ventricular pressure.

Sensitivity to settings of parameters in active stress model was investigated, since myofiber

contraction is the origin of both left ventricular pressure and radial wall stress [Eq. (7)], and thus of intramyocardial pressure and of coronary flow impediment. In both isovolumic and isobaric beats, NFA increases slightly if the twitch duration  $t_{max}$  [Eq. (12)] is reduced from 400 to 300 ms (Fig. 6, 2nd panel from top). Changing the linear relation between fiber stress and sarcomere shortening velocity into a hyperbolic one (by setting  $c_v = 1$  in Eq. (13)) does not affect NFA in isovolumic beats, where shortening velocity is zero. NFA in isobaric beats is hardly affected. Increasing the sarcomere length  $l_{s,a0}$ , below which active stress is zero [Eq. (11)], from 1.5 to 1.6  $\mu\text{m}$  yields a reduction in NFA in isovolumic and isobaric beats with a ventricular pressure below about 10 kPa (Fig. 6).

Sensitivity to coronary resistance was studied to mimic change in resistance due to variation in perfusion pressure. A two-fold simultaneous increase or decrease of all resistances in the coronary circulation model ( $R_{art,c}$ ,  $R_{myo,1}$ ,  $R_{myo,2}$  and  $R_{ven,c}$ ) does affect NFA more in isovolumic beats than in isobaric beats (Fig. 6, 3rd panel from top). Still, changes in NFA are limited, and pulsatility at low pressures is maintained.

Finally, sensitivity to myocardial compliance  $C_{myo,c}$  was studied, since pulsatility of coronary inflow is closely related to changes in coronary volume. When myocardial compliance  $C_{myo,c}$  is set to twice or half its reference value, NFA-values change quantitatively, but the phasic nature of coronary flow at low left ventricular pressure remains, both in isovolumic and



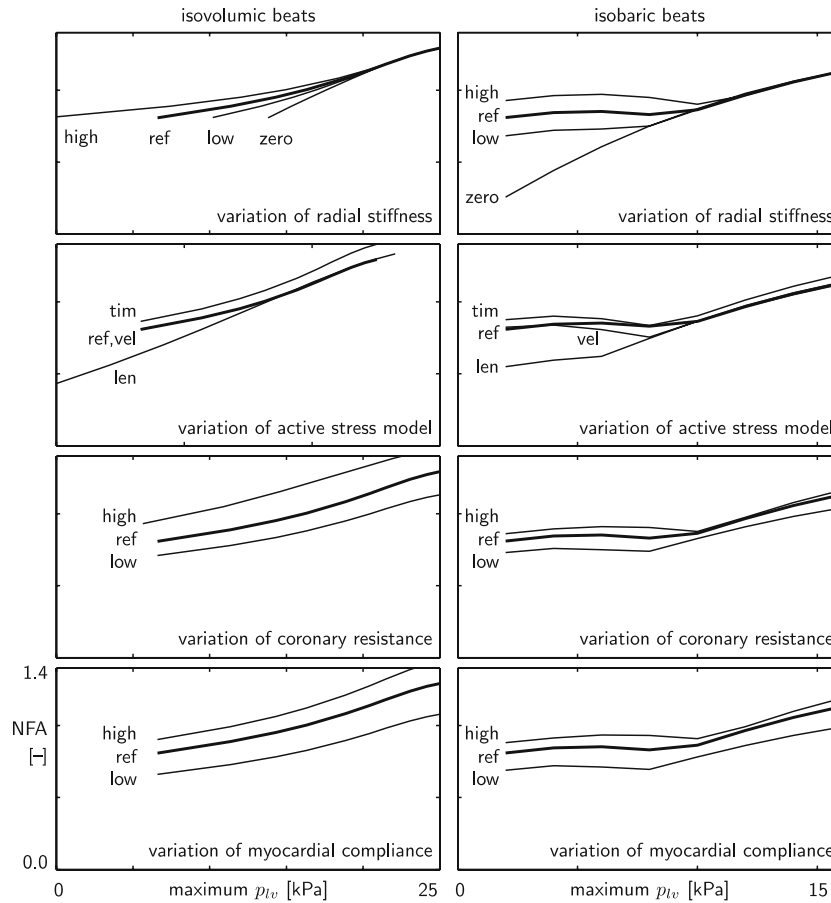


**FIGURE 6.** Sensitivity of relation between maximum left ventricular pressure and normalized flow amplitude (NFA) to settings of model parameters, for isovolumic beats (left) and isobaric beats (right). Results for reference parameter settings are indicated with ‘ref’. Top: radial stiffness parameter  $c_{r0}$  set to twice (‘high’) or half (‘low’) the reference value, or set to zero (‘zero’). Next: variation of active stress model: twitch duration reduced from 400 to 300 ms (‘tim’), stress–velocity relation changed from linear into hyperbolic (‘vel’), and stress-free sarcomere length increased from 1.5 to 1.6  $\mu\text{m}$  (‘len’). Next: all coronary resistances  $R_{\text{art},c}$ ,  $R_{\text{myo},1}$ ,  $R_{\text{myo},2}$  and  $R_{\text{ven},c}$  set to twice (‘high’) or half (‘low’) their reference values. Bottom: coronary myocardial capacitance  $C_{\text{myo},c}$  set to twice (‘high’) or half (‘low’) the reference value.

isobaric beats (Fig. 6, bottom panel). Again, the effect is larger in isovolumic beats than in isobaric beats.

## DISCUSSION

### Model Setup

The aim of this study was to design a model with a limited number of parameters for investigation of the primary relations between left ventricular pressure and volume, wall stress in fiber and transverse direction, intramyocardial pressure and the coronary blood flow. Central to the model are Eq. (7), which shows how fiber stress, that ultimately drives the cardiac cycle, is converted into both LV pressure and radial wall stress, and Eq. (17), that describes how LV pressure and radial wall stress contribute to intramyocardial pressure. Finally, it is the variation of intramyocardial

pressure that causes a variation in arterial coronary inflow through a change in coronary volume, represented by intramyocardial compliance. Since the use of a simple model is not without danger, we will address the impact of the main model simplifications.

In the model of ventricular wall mechanics spatial homogeneity of fiber stress and strain was assumed. The plausibility of this assumption has been illustrated in finite element models of ventricular mechanics.<sup>21,24</sup> The assumption that in plane stress is dominated by fiber stress [Eq. (3)] is realistic during systole, when myofibers are active and the main flow impediment occurs. Obviously, radial wall stress is spatially inhomogeneous, since the ventricle is thick walled. Yet we introduced a representative stress  $\bar{\sigma}_{m,r}$ , computed at a representative radial position enclosing one third of the wall volume, in evaluating the integral of  $\sigma_{m,r}$  over the wall thickness [Eq. (6)]. In principle, since the

transmural variation of radial strain is known once LV cavity volume is known, using the constitutive Eq. (15), the integral in Eq. (6) can be determined exactly. Due to the strong increase of radial wall strain from the outside to the inside surface and the nonlinearity of the constitutive law, its value would be dominated by the inner layers. However, in those layers the assumption of a solid wall with a smooth endocardial surface is in error: the endocardial surface shows many invaginations, relieving any radial stress that would build up in the subendocardial tissue. The choice to use representative positions, strains and stresses is compatible with the aim of the study, to investigate determinants of the coronary flow signal. Obviously the model cannot describe spatial differences in coronary perfusion,<sup>4</sup> which are clinically relevant in relation to vulnerability to ischemia.<sup>10</sup> In view of the use of a representative intramyocardial pressure, and the use of average values for the coronary compliances and resistances, the flow in the model should be regarded as a mean flow over the myocardial wall.

In the constitutive model for the cardiac tissue, the description of the active stress component is chosen as simple as possible, while maintaining the basic dependence of active stress on time, sarcomere length, and sarcomere shortening velocity. Within the limitations of the model, parameter settings are chosen to mimic experimental data.<sup>8,13</sup> The model could be extended to incorporate the sigmoidal relation between stress and sarcomere length, or the increase of twitch duration with increasing sarcomere length. However, we prefer the current version with a limited number of parameters, in view of the sensitivity analysis. The model for passive tissue stress is simplified, since we do not model a complete three-dimensional state of stress. Yet, the behavior shown in Fig. 1 agrees well with experimental data.<sup>28</sup>

We approximate extravascular pressure by intramyocardial pressure, thus neglecting the contribution of local tissue stress.<sup>26</sup> In fact this assumption is made in many other models, including the waterfall model,<sup>9</sup> the intramyocardial pump model,<sup>1,2,6,22</sup> and the models by Huyghe *et al.*<sup>12</sup> and Beyar *et al.*<sup>5,22,30</sup> In addition, in our model intramyocardial pressure is determined completely by the model of LV wall mechanics. Thus, we can not replicate the observation that intramyocardial pressure depends on perfusion pressure.<sup>18</sup> We feel this simplification is allowed in our simulations of isovolumic and isobaric beats, in which we assumed a constant perfusion pressure.

In the coronary circulation model resistances are constant. This is an approximation to the real situation, in which vessel diameter and therefore vessel resistance depend on vessel transmural pressure. The nature of the approximation is two-fold. First, we ne-

glect the chronic change in resistance due to a chronic change in perfusion pressure. This is not critical for the value of NFA, as is apparent from our sensitivity analysis where we applied a two-fold change of coronary resistance (Fig. 6). Second, we neglect cyclic changes in resistance during the cardiac cycle, which seems incompatible with the ability in the model to temporarily store blood in the coronary capacitance. Yet, the phasic nature of coronary flow is reproduced in the model. We explain this by noting that a change in vessel diameter during the cardiac cycle is associated with change in coronary volume, that affects coronary inflow irrespective of the location in the coronary tree where the volume change takes place. However, the associated change in resistance is important in the smallest vessels only, due to the nonlinear relation between vessel diameter and resistance. Obviously, the effect of changes in coronary resistance during the cycle may show up in aspects of the coronary flow signal, that are not captured by the normalized flow amplitude NFA.

The simplifications in the model may be seen as limitations, if one has the goal to explain all experimental observations available. In this study, we consider it a strength of the model, in view of our aim to investigate primary interactions and dependence on parameter settings.

### Results

In contrast to the situation in all other organs, coronary inflow of the heart muscle occurs mainly in diastole and is significantly impeded in systole. Experimentally, the amplitude of the coronary inflow signal was found to be only weakly coupled to systolic LV pressure in isovolumic beats at various LV volumes.<sup>15</sup> This behavior is illustrated by the three fits to experimental data sets, shown in top left panel of Fig. 5. As in the experiment, in our model pulsatility of coronary inflow is maintained at low left ventricular pressure, although dependence of NFA on pressure is slightly higher than in the experiment.

The mechanism by which pulsatility of coronary inflow is maintained in isovolumic beats is explained as follows (Fig. 4, left panel). Total LV pressure is the sum of diastolic pressure in the passive ventricle, and the extra pressure, generated by muscle contraction. Diastolic pressure decreases with decreasing volume and becomes negative as volume decreases below the resting volume of 60 ml. We note that in the experiments by Krams *et al.* negative diastolic pressure was induced as well, by applying suction to the balloon, inserted in the LV cavity.<sup>16</sup> Since LV volume is constant during a beat, radial wall stress and its contribution to LV pressure are constant as well. The extra pressure, related to

muscle contraction, reduces with decreasing volume, but at the lowest volume of 20 ml it still is about 15 kPa, and maximum total LV pressure is still about 11 kPa. The fact that the variation in LV pressure, which determines pulsatility of coronary flow, decreases more slowly with decreasing volume than maximum LV pressure, is reflected in the value of NFA shown in Fig. 5.

The relation between maximum LV pressure and minimum coronary inflow, shown in the bottom left panel of Fig. 5, qualitatively corresponds with experimental data by Kouwenhoven *et al.*<sup>14</sup> and Pagliaro *et al.*<sup>20</sup> In the latter study, minimum coronary inflow was found to decrease with increasing maximum LV pressure for pressures above 13 kPa, but was virtually independent of systolic LV pressure below 13 kPa. It was suggested that at low pressures ‘the shielding effect of the contracting ventricle prevents ventricular pressure from being transmitted in the myocardial wall’.<sup>20</sup> In our model, this shielding effect is identified as radial wall stress.

Experimentally, NFA in isobaric beats at low LV pressure was found to be about equal to NFA in isovolumic beats.<sup>15</sup> This finding is replicated in our model (Fig. 5, right panel). In contrast to the isovolumic case, the relation between maximum pressure and NFA is non monotonous, with distinct behavior at high and low pressures. At high pressures, LV volume remains mostly above the passive resting volume of 60 ml, and intramyocardial pressure is dominated by LV pressure. At low pressures, the LV ejects to far below the passive resting volume of 60 ml, and the decreasing contribution of LV pressure to intramyocardial pressure is compensated by the increasing contribution of radial wall stress.

It is to be noted that in the isobaric beats both contributions to intramyocardial pressure, radial wall stress and left ventricular pressure, vary in time, while in the isovolumic beats radial wall stress is constant and cyclic flow impediment is due to the varying contribution of left ventricular pressure only (Fig. 4). This explains the two peaks in the intramyocardial pressure-signal in Fig. 4: the first one is related to the rise in left ventricular pressure, while the second one arises from the rise in radial wall stress, related to the decrease in left ventricular volume.

Another experimental observation is that NFA is about proportionally related to LV contractility, expressed by maximum elastance, NFA being about zero when contractility was about zero.<sup>17</sup> This observation is replicated by our model, in which NFA changes about proportionally with the contractility parameter  $c$ , irrespective of the volume setting (Fig. 5). For low contractilities, minimum coronary inflow approaches the theoretical value of  $8.3 \text{ ml s}^{-1} 100 \text{ g}^{-1}$  of tissue,

obtained from the coronary perfusion pressure of 10 kPa, the total coronary resistance of  $6 \times 10^8 \text{ Pa s m}^{-3}$ , and a wall volume of 200 g.

Finally, it has been observed that intramyocardial pressure may exceed left ventricular pressure in low afterload beats.<sup>18</sup> This is also the case in our model (Fig. 4, right panel), and explained again from the contribution of radial wall stress at the low ventricular volumes associated with the low LV ejection pressures.

### Sensitivity Analysis

Sensitivity of NFA to the radial stiffness parameter  $c_{r0}$  in isovolumic beats is low (Fig. 6, top left). This can be best understood from Eq. (17), which shows that only the constant level of radial wall stress is affected by changing  $c_{r0}$ , while the variation of left ventricular pressure, and thus of intramyocardial pressure and arterial inflow, is unaffected. The increase in left ventricular pressure with decreasing stiffness is explained from Eq. (7), which shows that fiber stress is converted into both LV pressure and radial wall stress. With decreasing radial stiffness, an increasing part of fiber stress is converted into LV pressure. In the extreme case of zero radial stiffness, minimum left ventricular pressure is about 14 kPa, which is higher than the pressure measured in the experiment (Fig. 6).<sup>15</sup>

Variation of NFA with radial stiffness is more prominent in isobaric beats at low LV pressure (Fig. 6, top right). An increase of radial stiffness causes a more rapid increase of radial wall stress with decreasing volume below the equilibrium volume. Thus the pressure at which the contribution of radial wall stress to intramyocardial pressure takes over from the contribution of ventricular pressure is increased (17), and pulsatility of coronary inflow is maintained. At zero radial stiffness, intramyocardial pressure is determined fully by left ventricular pressure, explaining loss of pulsatility of coronary flow with decreasing ejection pressure, in disagreement with experimental findings.<sup>15</sup>

Sensitivity of NFA to settings of the active stress model (Fig. 6) is low, as far as the velocity and time dependence is concerned. NFA was more affected by increasing the stress-free sarcomere length from 1.5 to 1.6  $\mu\text{m}$ . In fact this variation has the same effect as decreasing contractility at low sarcomere lengths. Thus, in this case the decrease of NFA is explained from the decrease in variation of left ventricular pressure, which is reflected in a decreased variation of intramyocardial pressure.

The increase of NFA with increasing myocardial compliance (Fig. 6), both in isovolumic and isobaric beats, is explained from the fact that, at the same variation of intramyocardial pressure, the volume change of the myocardial bed increases. Hence the pulsatility of

arterial inflow is increased as well. A decrease of myocardial compliance has the opposite effect.

The first order effect of a variation of coronary resistance is a change in both the average and pulsatile component of coronary flow, as was illustrated already in Fig. 3. In this approximation, the relative changes in average and pulsatile flow component are equal, causing NFA to remain unaffected. However, since coronary compliance is kept constant, the relative contribution of flow related to volume change of the coronary bed becomes less when decreasing coronary resistance, causing the decrease of NFA, observed in Fig. 6. Increasing coronary resistance has the opposite effect.

#### *Relation with Other Models*

In comparison to the waterfall model<sup>9</sup> and the intramyocardial pump model,<sup>1,2,6,22</sup> our model is more advanced in its description of intramyocardial pressure, adding the effect of radial wall stress. Radial wall stress becomes important only below the zero-pressure volume of the passive ventricle. Thus, the early models still are applicable in normal physiological conditions, in which ventricular volume is higher than this zero-pressure volume during the major part of the cardiac cycle.

In comparison to the models by Beyar *et al.*<sup>5,29,30</sup> our model is simpler, emphasizing primary interactions, at the cost of information on transmural variation of coronary flow and long-term exchange of fluid between the coronary vessels and the interstitium. However, the reduced complexity yields increased insight into primary determinants of coronary flow impediment.

Main limitation of our model with respect to the model presented by Vis *et al.*,<sup>26,27</sup> lies in neglecting the direct contribution of tissue stress to the extravascular pressure and effective compliance of the coronary vessel. The approach of Vis *et al.* requires a detailed analysis of the equilibrium between the pressure in a cavity in the LV wall, and the stress in the surrounding tissue. However, such an analysis would compromise the simplicity, that we aim for in this study.

#### *Conclusion*

In conclusion, a mathematical model of the interaction between coronary flow and cardiac mechanics is presented, with a limited number of model parameters. The model replicates the experimental observations, that the phasic character of coronary inflow is virtually independent of maximum left ventricular pressure, that the amplitude of the coronary flow signal depends linearly on cardiac contractility, and that

intramyocardial pressure in the left ventricular wall may exceed left ventricular pressure. The normalized amplitude of coronary inflow is mainly determined by contractility, reflected in dependence of active fiber stress on sarcomere length, and maintained at low ventricular volumes by radial wall stress. The sensitivity of the NFA to myocardial coronary compliance and resistance, and to the relation between active fiber stress, time, and sarcomere shortening velocity is low.

#### REFERENCES

- <sup>1</sup>Arts, T. A mathematical model of the dynamics of the left ventricle and the coronary circulation. PhD Thesis, University of Limburg, Maastricht, The Netherlands, 1978.
- <sup>2</sup>Arts, T. and R. S. Reneman Interaction between intramyocardial pressure (IMP) and myocardial circulation. *J. Biomech. Eng.* 107:51–56, 1985.
- <sup>3</sup>Arts, T., P. H. M. Bovendeerd, F. W. Prinzen, and R. S. Reneman Relation between left ventricular cavity pressure and volume and systolic fiber stress and strain in the wall. *Biophys. J.* 59:93–102, 1991.
- <sup>4</sup>Bassingthwaight, J. B., D. A. Beard, and Z. Li The mechanical and metabolic basis of myocardial blood flow heterogeneity. *Basic Res. Cardiol.* 96:582–594, 2001.
- <sup>5</sup>Beyar, R., R. Ben-Ari, C. A. Gibbons-Kroeker, J. V. Tyberg, and S. Sideman Effect of interconnecting collagen fibers on left ventricular function and intramyocardial compression. *Cardiovasc. Res.* 27:2252–2263, 1993.
- <sup>6</sup>Bruinsma, P., T. Arts, J. Dankelman, and J. A. Spaan Model of the coronary circulation based on pressure dependence of coronary resistance and compliance. *Basic Res. Cardiol.* 83:510–524, 1988.
- <sup>7</sup>Chilian, W. M., S. M. Layne, E. C. Klausner, C. L. Eastham, and M. L. Marcus Redistribution of coronary microvascular resistance produced by dipyridamole. *Am. J. Physiol.* 256:H383–H390, 1989.
- <sup>8</sup>de Tombe, P. P. and H. E. D. J. ter Keurs Sarcomere dynamics in cat cardiac trabeculae. *Circ. Res.* 68:588–596, 1991.
- <sup>9</sup>Downey, E. M. and E. S. Kirk Inhibition of coronary blood flow by a vascular waterfall mechanism. *Circ. Res.* 34:251–257, 1975.
- <sup>10</sup>Fokkema, D. S., J. W. Van Teeffelen, S. Dekker, I. Vergroesen, J. B. Reitsma, and J. A. Spaan Diastolic time fraction as a determinant of subendocardial perfusion. *Am. J. Physiol.* 288:H2450–H2456, 2005.
- <sup>11</sup>Giezeman, M. J., E. van Bavel, C. A. Grimbergen, and J. A. Spaan Compliance of isolated porcine coronary small arteries and coronary pressure-flow relations. *Am. J. Physiol.* 267:H1190–H1198, 1994.
- <sup>12</sup>Huyghe, J. M., T. Arts, D. H. van Campen, and R.S. Reneman Porous medium finite element model of the beating left ventricle. *Am. J. Physiol.* 262:H1256–H1267, 1992.
- <sup>13</sup>Janssen, P. M. and W. C. Hunter Force, not sarcomere length, correlates with prolongation of isosarcometric contraction. *Am. J. Physiol.* 269:H676–H685, 1995.
- <sup>14</sup>Kouwenhoven, Ee, I. Vergroesen, Yi Han, and J. A. Spaan Retrograde coronary flow is limited by time-varying elastance. *Am. J. Physiol.* 263:H484–H490, 1992.

- <sup>15</sup>Krams, R., P. Sipkema, and N. Westerhof Varying elastance concept may explain coronary systolic flow impediment. *Am. J. Physiol.* 257:H1471–H1479, 1989.
- <sup>16</sup>Krams, R., P. Sipkema, J. Zegers, and N. Westerhof Contractility is the main determinant of coronary systolic flow impediment. *Am. J. Physiol.* 257:H1936–H1944, 1989.
- <sup>17</sup>Krams, R., A. C. T. A. van Haelst, P. Sipkema, and N. Westerhof Can coronary systolic–diastolic flow differences be predicted by left ventricular pressure or time-varying intramyocardial elastance?. *Basic Res. Cardiol.* 84:149–159, 1989.
- <sup>18</sup>Mihailescu, L. S. and F. L. Abel Intramyocardial pressure gradients in working and nonworking isolated cat hearts. *Am. J. Physiol.* 266:H1233–H1241, 1994.
- <sup>19</sup>Nikolić, S., E. L. Yellin, K. Tamura, H. Vetter, T. Tamura, J. S. Meisner, and R. W. M. Frater Passive properties of canine left ventricle: Diastolic stiffness and restoring forces. *Circ. Res.* 62:1210–1222, 1988.
- <sup>20</sup>Pagliari, P., D. Gattullo, R. J. Linden, G. Losano, and N. Westerhof Systolic coronary flow impediment in the dog: Role of ventricular pressure and contractility. *Exp. Physiol.* 83:821–831, 1998.
- <sup>21</sup>Rijcken, J., P. H. M. Bovendeerd, A. J. G. Schoofs, D. H. van Campen, and T. Arts Optimization of cardiac fiber orientation for homogeneous fiber strain during ejection. *Ann. Biomed. Eng.* 27:289–297, 1999.
- <sup>22</sup>Spaan, J. A., N. P. Breuls, and J. D. Laird Diastolic–systolic coronary flow differences are caused by intramyocardial pump action in the anesthetized dog. *Circ. Res.* 49:584–93, 1981.
- <sup>23</sup>Spaan, J. A. E. Coronary diastolic pressure–flow relation and zero flow pressure explained on the basis of intramyocardial compliance. *Circ. Res.* 56:293–309, 1985.
- <sup>24</sup>Vendelin, M., P. H. M. Bovendeerd, J. Engelbrecht, and T. Arts Optimizing ventricular fibers: Uniform strain or stress, but not ATP consumption, leads to high efficiency. *Am. J. Physiol.* 283:H1072–H1081, 2002.
- <sup>25</sup>Vis, M. A., P. Sipkema, and N. Westerhof Modeling pressure–flow relations in cardiac muscle in diastole and systole. *Am. J. Physiol.* 272:H1516–H1526, 1997.
- <sup>26</sup>Vis, M. A., P. H. M. Bovendeerd, P. Sipkema, and N. Westerhof Effect of ventricular contraction, pressure, and wall stretch on vessels at different locations in the wall. *Am. J. Physiol.* 272:H2963–H2975, 1997.
- <sup>27</sup>Vis, M. A., P. Sipkema, and N. Westerhof Compression of intramyocardial arterioles during cardiac contraction is attenuated by accompanying venules. *Am. J. Physiol.* 273:H1003–H1011, 1997.
- <sup>28</sup>Yin, F. C. P., R. K. Strumpf, P. H. Chew, and S. L. Zeger Quantification of the mechanical properties of noncontracting canine myocardium under simultaneous biaxial loading. *J. Biomech.* 20:577–589, 1987.
- <sup>29</sup>Zinemanas, D., R. Beyar, and S. Sideman Effects of myocardial contraction on coronary blood flow: An integrated model. *Ann. Biomed. Eng.* 22:638–652, 1994.
- <sup>30</sup>Zinemanas, D., R. Beyar, and S. Sideman An integrated model of LV muscle mechanics, coronary flow, and fluid and mass transport. *Am. J. Physiol.* 268:H633–H644, 1995.